



Seismo-geomagnetic anomalies and $M \geq 5.0$ earthquakes observed in Taiwan during 1988–2001

J.Y. Liu ^{a,b,*}, C.H. Chen ^c, Y.I. Chen ^d, H.Y. Yen ^c, K. Hattori ^e, K. Yumoto ^f

^a Institute of Space Science, National Central University, Chung-Li 32054, Taiwan

^b Center for Space and Remote Sensing Research, National Central University, Chung-Li 32054, Taiwan

^c Institute of Geophysics, National Central University, Chung-Li 32054, Taiwan

^d Institute of Statistics, National Central University, Chung-Li 32054, Taiwan

^e Marine Biosystems Research Center, Chiba University, Chiba, Japan

^f Space Environment Research Center, Kyushu University, Japan

Accepted 6 February 2006

Available online 16 May 2006

Abstract

In this paper, a relationship between $M \geq 5.0$ earthquakes and diurnal variations of the total geomagnetic field recorded at eight magnetometers in Taiwan during 1988–2001 are examined. One magnetometer station was setup in a seismic quiet area as a reference, while the others were located in areas of high seismicity or crustal activity observing earthquake effects. We compute the distribution of diurnal range ratios between the reference and each observation station for the entire thirteen years as a background and compare it with the monitored distributions during five different time periods before and after an $M \geq 5.0$ earthquake occurring within a distance of 50 km from the observation station. Three specific earthquakes with different magnitudes, including the $M = 7.3$ Chi-Chi earthquake show that the monitored distributions one month before and during the month of the earthquakes significantly depart from the associated background. It is found that changes of underground conductivities and currents around the forthcoming epicenter significantly affect the near-by geomagnetic field on the ground during the earthquake preparation period. The statistical results demonstrate that the monitored distributions of geomagnetic anomalies are highly related to the focal mechanism.

© 2006 Published by Elsevier Ltd.

Keywords: Geomagnetism; Magnetic anomaly; Diurnal variations; Earthquake forecasts

1. Introduction

Many examples of geomagnetic changes associated with earthquakes have been reported (see papers listed in Hayakawa and Fujinawa, 1994; Hayakawa, 1999; Hayakawa and Molchanov, 2002). Chen et al. (2004) found that temporal changes of geomagnetic field recorded near coming epicenters tended to be constants and that the associated annual change rate approached a small value, from few months to two years before large earthquake occurrences. These

long-term datasets are certainly essential for exploring the relationship between geomagnetic changes and earthquake occurrences. However, their shortcoming is the data sampling rate being generally too low for detailed quantitative analysis.

By contrast, a good deal of researches on geomagnetic variations in the ultra-low-frequency (ULF) ranges associated with large earthquakes has been reported (see papers listed in Hattori, 2004). The results show that ULF geomagnetic anomalies possibly appear within a distance of 50–100 km from forthcoming epicenters several hours to few months prior to large earthquakes. Although there appeared many such convincing evidence, the ULF analysis requires rather sophisticated signal processing and relatively high data sampling rate.

* Corresponding author. Address: Institute of Space Science, National Central University, Chung-Li 32054, Taiwan. Tel.: +886 3 4228374; fax: +886 3 4334394.

E-mail address: jyliu@jupiter.ss.ncu.edu.tw (J.Y. Liu).

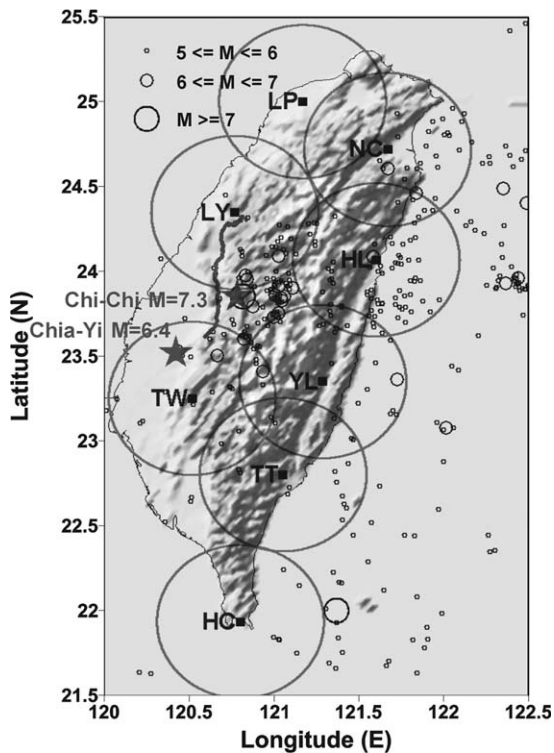


Fig. 1. Locations of the $M \geq 5.0$ earthquakes, of the Chelungpu fault, and of the eight magnetometers during 1988–2001. The curve between LY and TW stations is the Chelungpu fault and the circles denote the radius of 50 km from the magnetometers.

In this paper, we adapt the load–unload ratio introduced by Zeng et al. (2002) to study how the total geomagnetic field variations recorded with a moderate sampling rate of every 10 min at eight magnetometer stations are related to $M \geq 5.0$ earthquakes that occurred in Taiwan during 1988–2001 (Fig. 1).

2. Theory and methodology

An earthquake is one of the forms of intense mass motion in the Earth’s interior. Seismic activity itself depends on the structural condition, the medium deformation, and the cracking process inside the lithosphere and its source in the deeper layer, possibly modifies the under-

ground electrical structure and emits in the form of electromagnetic variations.

The geomagnetic deep sounding (GDS) method (Prasad et al., 1993; Prasad, 1999), which uses various frequencies of geomagnetic field as the signal source, has been employed to study the Earth’s electrical structure. The most powerful nature signal source (generator) is the solar wind, which constantly bombards the Earth’s magnetic field (for detail, see Kivelson and Russell, 1995). The balance place between the solar wind kinetic and the Earth’s magnetic field (magnetosphere) pressures is termed “the magnetopause”. When the solar wind compresses or decompresses the magnetosphere, the magnetopause moves toward (away from) the Earth generating numerous waves and then loads (unloads) a kinetic pressure/energy via the geomagnetic field on the Earth. The generated waves around the magnetopause travel from space down to the Earth. A magnetometer on the ground simultaneously registers both waves (signals) from space and their reflections together with seismo-generated signals from the Earth interior. Due to the Earth’s rotation, the solar wind compression and decompression resulting in the geomagnetic field recorded on the ground change diurnally. Fig. 2 displays the daily maximum (load) B_M , minimum (unload) B_m and their associated range $\Delta B (=B_M - B_m)$ of the geomagnetic total field (Chapman and Bartels, 1940; Parkinson, 1983) observed at Lunping (LP).

For two nearby (~ 100 km) magnetometers i and j signals generated by the solar wind are almost identical. Therefore, if the electrical structures under the magnetometers remain unchanged, the ratios between the two daily ranges $R_{ij} (= \Delta B_i / \Delta B_j)$ and/or $R_{ji} (= \Delta B_j / \Delta B_i)$ are a constant of about 1. The constant may be slightly greater and/or less than 1 which mainly depends on the relative geomagnetic latitudes of the two stations. Meanwhile, if the electrical structure under either one of the two magnetometers changes due to earthquake preparation processes, the ratio R_{ij} or R_{ji} then departs from 1. Therefore, we compute proportions of R_{ij} for $\Delta B_i < \Delta B_j$, $R_{ij} = R_{ji} = 1$, and R_{ji} for $\Delta B_j < \Delta B_i$ for the entire 13-year observation period to construct a background distribution for each station. We also apply a similar process for every contiguous 31-day to obtain a monitored distribution for each station. In partic-

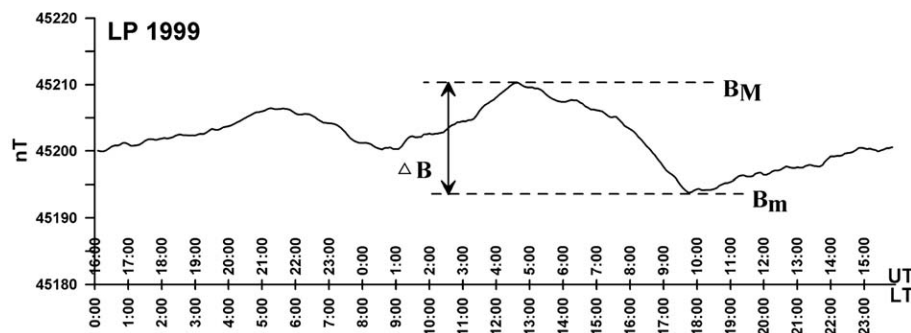


Fig. 2. Average curve of diurnal variations recorded at the LP station in 1999.

ular, we monitor the ratio distributions for coseismic effect five 31-day periods before and after the earthquake.

It is known that the diurnal magnetic total fields on the ground are changed mainly by the Chapman–Ferraro current at the magnetopause controlled by the solar wind compression (load) and rarefaction (unload), and the ring current in the magnetosphere during magnetic storms and substorms. A comparison shows that the background and monitored observations with and without removing the current effects are nearly identical, except that the disturbed solar wind, magnetic storm, and substorm related currents slightly increase the percentages of the peak of the background and monitored distributions. For simplicity, we use all the recorded data during the entire 13-year and 31-day to construct the background and monitored distributions, respectively.

For practical application, one magnetometer setup in a seismic quiet area provides a reference, while the other magnetometers are deployed at active regions observing geomagnetic changes. For each observation magnetometer, the diurnal ratios (both R_{ro} and R_{or} , where r and o denote the reference and the observation magnetometers, respectively) are derived and their distribution for the entire

13-year period is then computed as a background. Meanwhile, five distributions for 31 days centered at the earthquake occurrence as well as during 16–46 and 47–77 days before and after the earthquake occurring within a distance of 50 km to the observation magnetometer are employed to monitor seismo-geomagnetic anomalies. To investigate the relationship between the ratios and large earthquake occurrences in a seismic active region, the monitored distributions for the five time periods, which respectively stand for the month during as well as one and two month before and after the earthquake, are further compared to the associated background distribution.

Table 1
Locations of magnetometer stations

Station	Latitude (°N)	Longitude (°E)
Lunping (LP)	25.0	121.2
Neicheng (NC)	24.7	121.6
Liyutan (LY)	24.3	120.8
Hualien (HL)	24.1	121.6
Yuli (YL)	23.4	121.3
Tsengwen (TW)	23.3	120.5
Taitung (TT)	22.8	121.0
Hengchun (HC)	21.9	120.8

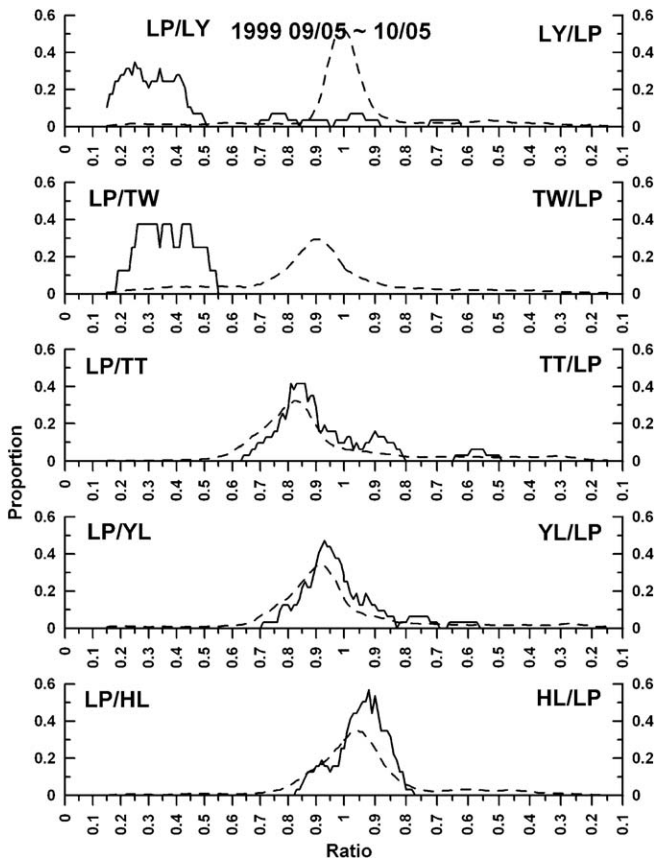


Fig. 3. The monitored distributions at each magnetometer station during the month of (15 days before and after) the Chi-Chi earthquake. The vertical axes are the distributions in number of proportion of the ratios, and the horizontal axes represent the ratios of R_{ro} and R_{or} . The background and monitored distributions are denoted by dashed and solid curves, respectively.

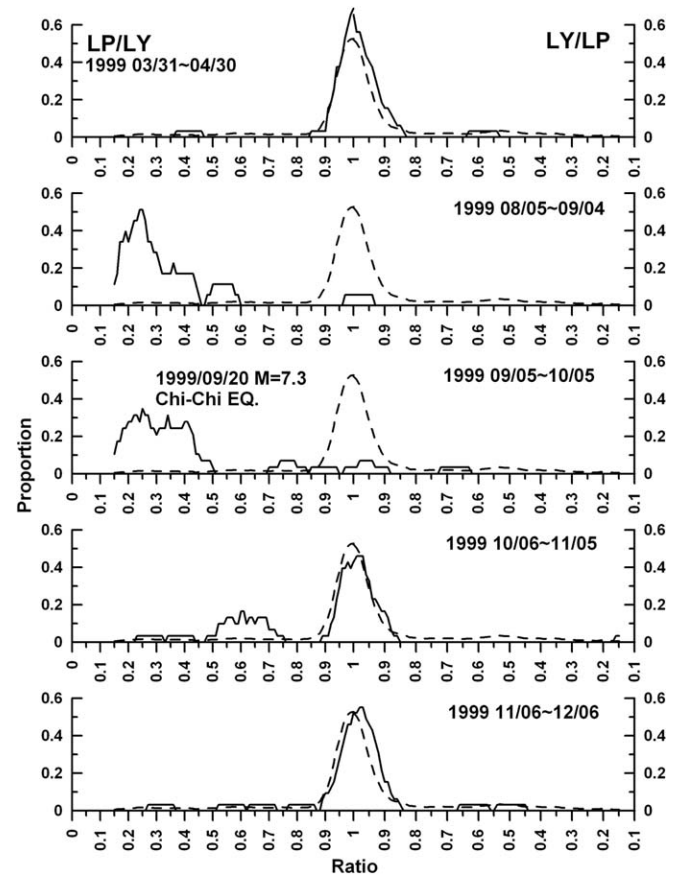


Fig. 4. The monitored distributions (solid curves) in five time periods of the Chi-Chi earthquake together with the background distribution (dashed curves) at the LY station.

3. Observation and interpretation

Taiwan is located in an active part of the Circum-Pacific seismic belt. The interaction between the northwestward moving Philippine sea plate and Eurasia plate depicts an intense and complicated geological structure, and results in large earthquakes in the Taiwan collision zone (Wang et al., 2002). Earthquakes in the Taiwan area are routinely documented and published by the Central Weather Bureau. Meanwhile, a network of eight magnetometers equipped with continuous recording systems was established in 1988 by the Institute of Earth Science, Academia Sinica to monitor the geomagnetic total field of Taiwan Island.

The island-wide geomagnetic network consists of eight stations (Fig. 1). A proton precession magnetometer (Geometrics Model G-856) with a 0.1 nT sensitivity and continuous recording system was used at each station. All stations were located in areas of high seismicity or crustal activity, except for the Luning (LP) station. The LP is located in a seismically quiet area in northern Taiwan and is considered to be a reference station. In other words, we assume that there is no stress factor to affect the geomagnetic intensity at the reference station. The Liyutan (LY) and the Tsengwen (TW) stations are located in western Taiwan. The other five stations, Neicheng (NC), Hua-

lien (HL), Yuli (YL), Taitung (TT), and Hengchun (HC), are distributed over eastern and southern Taiwan. Table 1 lists the locations of the eight magnetometers. The sampling rate at the LP is at 5 min, while other stations have 10 min intervals. The HC has many data gaps and therefore only the ratios of the six observing stations to the reference (LP) station are examined.

Let's take the Chi-Chi earthquake (M7.3, 20 September 1999) as the first example to see if the monitored distribution at each station during the earthquake is similar to its associated background distribution during 1988–2001. Owing to many data gaps also in NC during the event, we simply focus on measurements at the five high seismicity stations. Fig. 3 reveals during the month of the earthquake (9/5–10/5 1999) that the monitored distributions at the LY and TW significantly depart from their backgrounds. However, since the stations are relatively far away from the Chi-Chi epicenter and Chelungpu fault, the monitored distributions are similar to their backgrounds at the TT, YL and HL stations. We further study the monitored distributions at LY and TW during the five time periods of the Chi-Chi earthquake. Note that the LY station has a data gap during 5/1–8/4 1999. Fig. 4 illustrates at the LY that the monitored distributions one month before (8/5–9/4) and during the earthquake month significantly

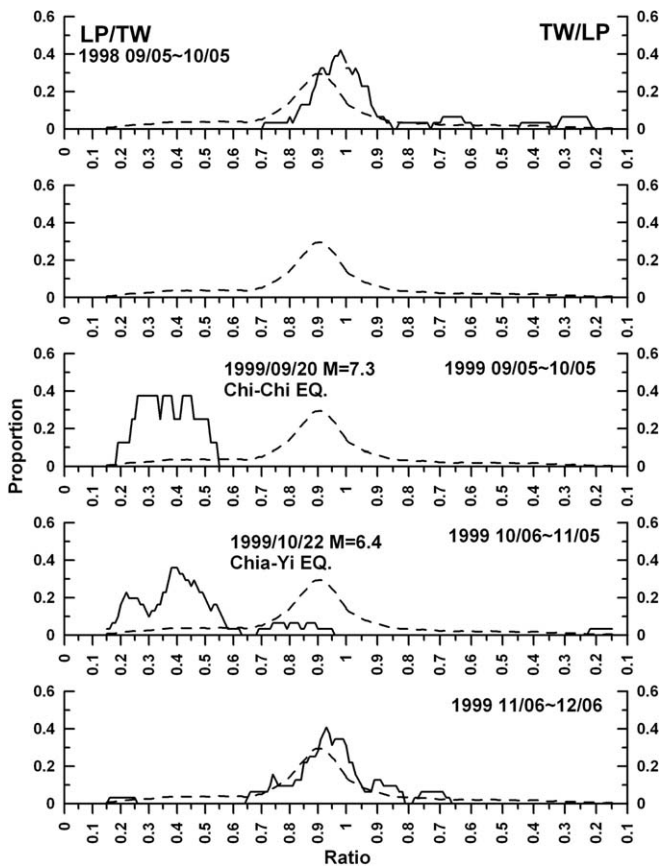


Fig. 5. The monitored distributions (solid curves) in five time periods of the Chi-Chi earthquake together with the background distribution (dashed curves) at the TW station.

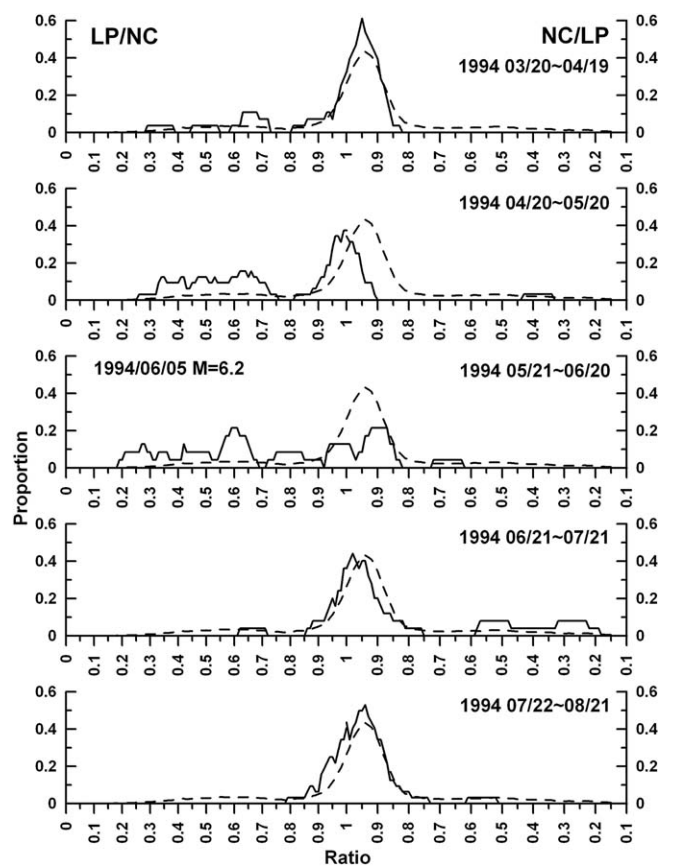


Fig. 6. The monitored distributions (solid curves) in five time periods of the 5 June 1994 M6.2 earthquake together with the background distribution (dashed curves) at the NC station.

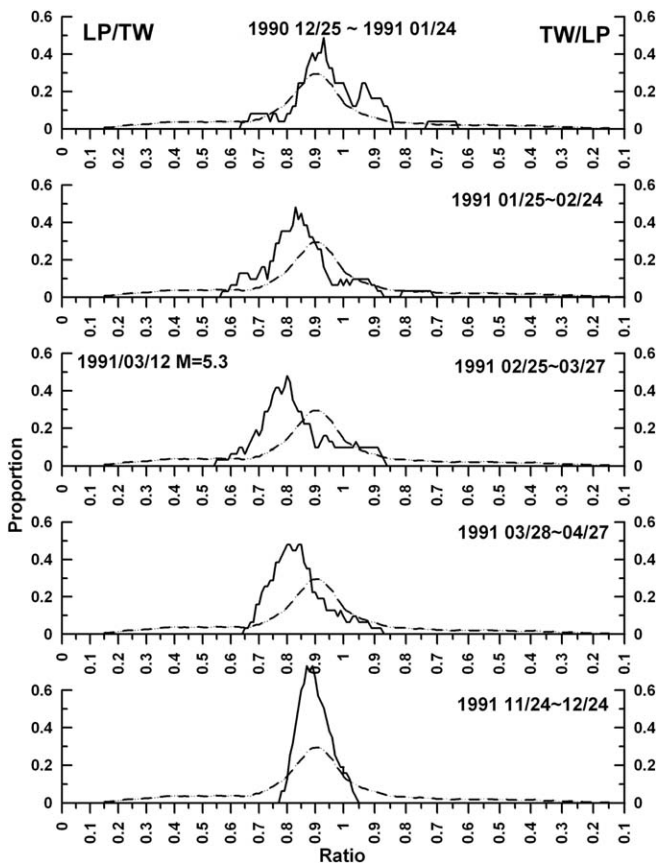


Fig. 7. The monitored distributions (solid curves) in five time periods of the 12 March 1991 M5.3 earthquake together with the background distribution (dashed curves) at the TW station.

depart from the background but the anomalies in the monitored distribution one month after the earthquake (10/6–11/5) become much less. Moreover, the monitored distributions five months before (3/31–4/30) and two months after (11/6–12/6) the earthquake are generally similar to the background. Meanwhile, the TW station had not been operated since 1 year before the Chi–Chi earthquake but was quickly restored right after. Fig. 5 displays that the monitored distribution long before the earthquake (9/5–10/5, 1998) is similar to the background, but during the earthquake significantly departs from the background and two months after the earthquake become similar again. The monitored distribution at the TW, in comparison with that at the LY, still significantly departs from the associated background one month after the Chi–Chi earthquake. This might be due to the fact that, following the Chi–Chi earthquake, the M6.4 Chia-Yi earthquake that occurred on 22 October 1999 is very close to the TW station.

We also arbitrarily select two more examples of $M \geq 6.0$ and $M \geq 5.0$ earthquakes. Fig. 6 depicts another example that at the NC station the monitored distributions two months before as well as one and two months after are similar to the associated background, but the monitored distributions one month before and during the M6.2, 5 June 1994 earthquake, apparently depart from the back-

ground. The other example illustrates the 12 March 1991 M5.3 earthquake that occurred near the TW station. Again, it can be seen in Fig. 7 that the monitored distributions one month before and after deviate from the background, but the monitored distributions two months before and after are similar to the background.

For a statistical analysis, the monitored distributions are computed in the five time periods for each $M \geq 5.0$ earthquake occurring within a distance 50 km from the observation magnetometer stations at the six high seismicity areas. We compare them with their associated backgrounds and find that anomalies generally appear in the monitored distributions one month before and during the month of the earthquake occurrences (Fig. 8). Fig. 8(a) and (b) illustrate that anomalies of the monitored distributions at the LY and TW stations occur mainly in left side of the associated background. This indicates that in western Taiwan the diurnal geomagnetic variations anomalously increase one month before the earthquakes. Fig. 8(c) and (d) reveal that the anomalies of the monitored distributions at the NC and HL stations occur in either side of the associated backgrounds. It shows that in northeastern Taiwan the diurnal geomagnetic variations anomalously either increase or decrease one month before the earthquakes. For Fig. 8(e) and (f), the anomalies of the monitored distributions at the YL and TT stations occur mainly in the right side of the associated backgrounds, which suggest that the diurnal geomagnetic variations anomalously decrease one month before the earthquakes in eastern Taiwan. The proportions of the monitored distributions with anomalies before and during the 65 $M \geq 5.0$ and 8 $M \geq 6.0$ earthquakes observed at the six magnetometer stations are 75.4% (=49/65) and 87.5% (=7/8), respectively. This suggests that for the greater earthquakes there is a better chance observing anomalies in the monitored distributions during and one month before the earthquake.

4. Discussion and conclusion

It has been shown that the anomalies of monitored distributions at the LY and TW stations occurred in left side of the associated backgrounds, which corresponds to a significant increase in the diurnal range of the geomagnetic field variations one month before and during the Chi–Chi and Chia-Yi earthquakes. These anomalous features indicate that the underground conductivity increases and/or current enhances near the LY and TW stations. Chen and Chen (2000) observed a low resistivity anomaly which is less than $10 \Omega \text{ m}$ with a depth ranging about 10–15 km below the hypocenter during the Chi–Chi earthquake. They suggest the low resistivity anomaly to be related to underground fluids or water. Note that before the large earthquake, the fluid expanded or compressed in the crust results in the change of underground conductivity and current. These in turn modify the geomagnetic field around the coming earthquake area. The agreement between our study and the resistivity study (Chen and Chen, 2000) during the

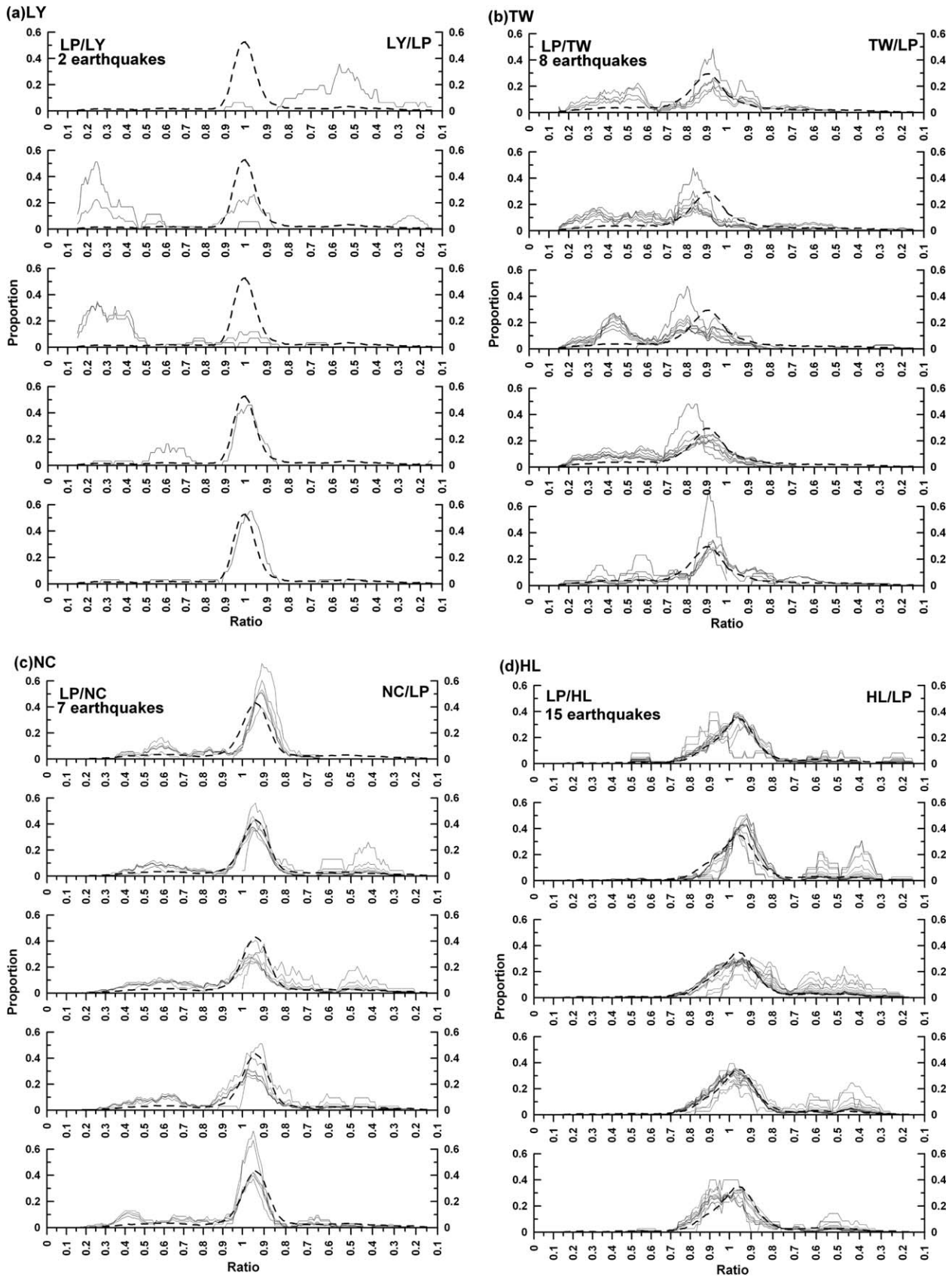


Fig. 8. The over-layer plots of the monitored distributions in five time periods of the $M \geq 5.0$ earthquake (thin solid curves) and their associated background (heavily dashed curves) at the six stations during 1988–2001. The distributions at LY, TW, NC, HL, and YL, TT are denoted with (a)–(f), respectively.

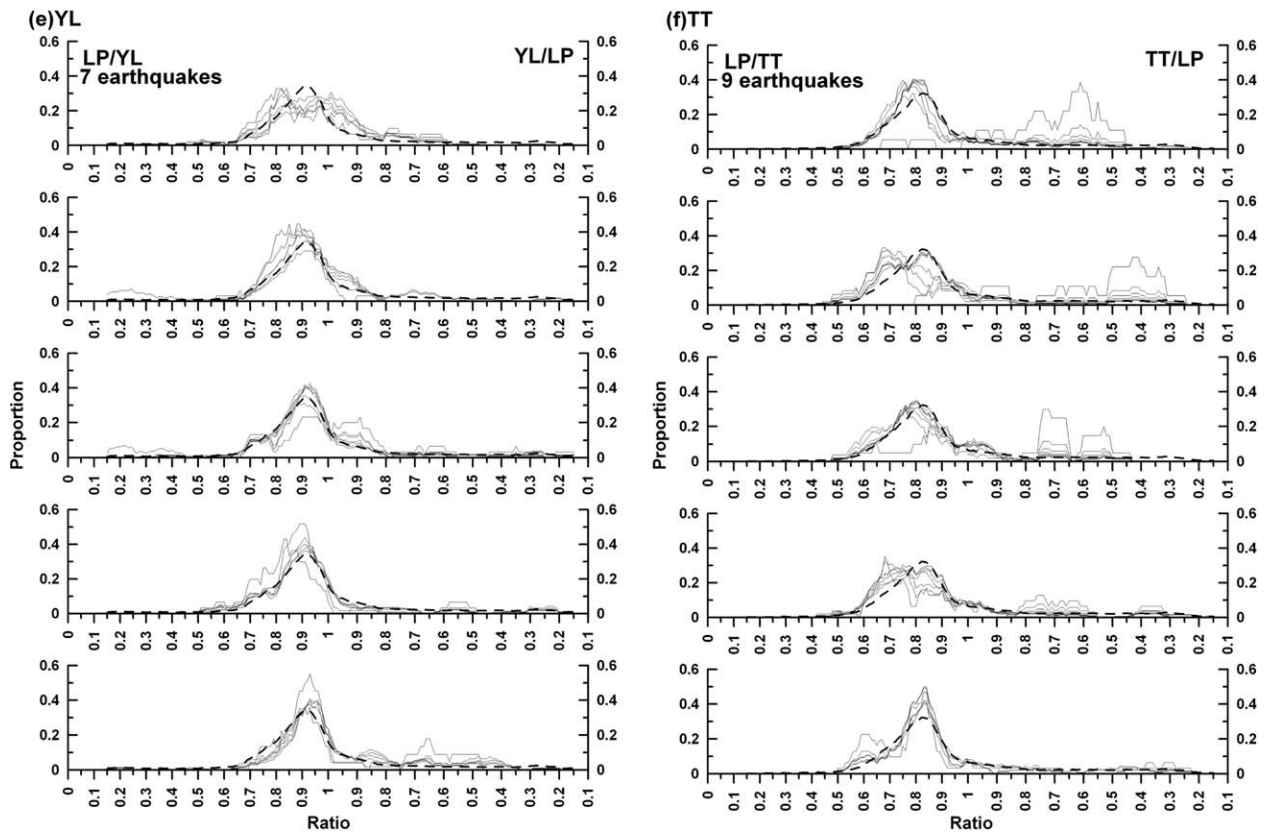


Fig. 8 (continued)

Chi-Chi earthquake indicates that the anomalies in the diurnal geomagnetic range resulted from nearby underground conductivity and current changes.

Both the three case studies and statistical analyses show that the geomagnetic anomalies appear one month before and during the earthquakes. The statistical results further reveal that the anomalies of the monitored distributions in western, eastern, and northeastern Taiwan resulted, respectively, resulted from increase, decrease, and mixture of increase and decrease in the diurnal range of geomagnetic variations. Coincidentally, it is known that the focal mechanisms in western, eastern and northeastern Taiwan are the reversed fault, strike-slip, and complex, respectively (Yeh et al., 1991). This coincidence indicates that the reverse and strike-slip faults result in the underground conductivity and/or the diurnal range of the magnetic variations on the ground near the forthcoming epicenter increase and decrease, respectively.

Acknowledgements

The earthquake catalog is retrieved from the Central Weather Bureau of Taiwan. This research was supported by the Ministry of Education, Taiwan, under Grant 91-N-FA07-7-4 for the iSTEP project of the National Central University.

References

Chapman, S., Bartels, J., 1940. *Geomagnetism*. The Charendon Press, Oxford, 1049pp.

Chen, C.S., Chen, C.C., 2000. Magnetotelluric soundings of the source area of the 1999 Chi-Chi earthquake in Taiwan: evidence of fluids at the hypocenter. *Terr. Atmo. Ocean Sci.* 11, 679–688.

Chen, C.H., Liu, J.Y., Yen, H.Y., Zeng, X., Yeh, Y.H., 2004. Changes of geomagnetic total field and occurrences of earthquakes in Taiwan. *Terr. Atmo. Ocean Sci.* 15, 361–370.

Hattori, K., 2004. ULF Geomagnetic changes associated with large earthquakes. *Terr. Atmo. Ocean Sci.* 15, 329–360.

Hayakawa, M., Fujinawa, Y. (Eds.), 1994. *Electromagnetic Phenomena Related to Earthquake Prediction*. Terra Science Publishing Company, Tokyo, p. 677.

Hayakawa, M. (Ed.), 1999. *Atmospheric and ionospheric Electromagnetic Phenomena Associated with Earthquakes*. Terra Science Publishing Company, Tokyo, p. 996.

Hayakawa, M., Molchanov, O.A. (Eds.), 2002. *Seismo Electromagnetics: Lithosphere–Atmosphere–Ionosphere*. Terra Science Publishing Company, Tokyo, p. 477.

Kivelson, M.G., Russell, C.T., 1995. *Introduction to Space Physics*. Cambridge University Press, 433pp.

Parkinson, W.D., 1983. *Introduction to Geomagnetism*. Scottish Academic Press, Edinburgh and London, 588pp.

Prasad, S.N., 1999. An inversion of geomagnetic deep sounding data using simulated annealing. *Physics of the Earth and Planetary Interiors* 110, 129–135.

Prasad, S.N., Verma, S.K., Pek, J., Cerv, V., 1993. 2-D inversion of geomagnetic deep sounding data near Ujjain-Guna, India. *Geophys. J. Int.* 113, 767–775.

- Wang, C., Huang, C.P., Ke, L.Y., Chien, W.J., Hsu, S.K., Shyu, C.T., Cheng, W.B., Lee, C.S., Teng, L.S., 2002. Formation of the Taiwan Island as a solitary wave along the Eurasian continental plate margin: magnetic and seismological evidence. *Terr. Atmo. Ocean Sci.* 13, 339–354.
- Yeh, Y.H., Barrier, E., Lin, C.H., Angiler, J., 1991. Stress tensor analysis in the Taiwan area from focal mechanism of earthquakes. *Tectonophysics* 200, 267–280.
- Zeng, X., Liu, J.Y., Lin, Y., Xu, C., 2002. The evolution of dynamic imagines of geomagnetic field and strong earthquake. *J. Atmo. Elec.* 22, 191–205.